6. van der Stelt, J. M. & Koopmans-van Beinum, F. J. in *Precursors of Early Speech* (eds Lindblom, B. & Zetterstrom, R.) 163–173 (Stockton, New York, 1986).
7. Pinker, S. & Bloom, P. in *The Adapted Mind: Evolutionary Psychology and the Generation of Culture* (eds Barkow, J. H. *et al.*) 451–493 (Oxford Univ. Press, New York, 1992).
8. Jusczyk, P. W. *The Discovery of Spoken Language* (MIT Press, Cambridge, Massachusetts, 1997).
9. Vihman, M. M. *Phonological Development: The Origins of Language in the Child* (Blackwell, Cambridge, MA, 1996).
10. Petitto, L. A. & Marentette, P. F. *Science* **251,** 1493–1496 (1991).
11. Meier, R. P. & Willerman, R. in *Language, Gesture, and Space* (eds Emmorey, K. & Reilly, J. S.) 391–409 (Erlbaum, Mahwah, New Jersey, 1995).
12. Petitto, L. A. *et al. Proc. Natl Acad. Sci. USA* **97,** 13961–13966 (2000).


Spectrographic imaging

# A bird's-eye view of the health of coral reefs

Almost three-quarters of the world's coral reefs are thought to be deteriorating as a consequence of environmental stress. Until now, it has been possible to evaluate reef health only by field survey, which is labour-intensive and time-consuming. Here we map live coral cover from the air by remote imaging, a technique that will enable the state of shallow reefs to be monitored swiftly and over large areas.

It is predicted that coral reefs will suffer mounting stress associated with a global increase in atmospheric carbon dioxide over the coming decades[1,2] and from local disturbances such as overfishing[3] and disease[4]. The most obvious effect of such stress is a decline in living coral cover, so a temporal change in cover is a good indicator of the state of health of a coral reef. However, the measurement of coral cover by field survey[5] is impractical on the scale of hundreds to thousands of square kilometres.

Measurements of the reflected light spectra of reef biota and substrata indicate that the dominant groups can be distinguished *in situ*[6–10], but until now it has not been clear whether such spectral differences can be detected remotely from the air or from space. We acquired high-spatial-resolution (1 m × 1 m), multispectral images from the air of two reefs in the lagoon of Rangiroa Atoll, French Polynesia, by using a compact spectrographic imager. We carried out this imaging in November 1998 because coral populations had suffered significant mortality after the extreme El Niño/Southern Oscillation that occurred in the austral summer of 1997–98 (ref. 11). At the same time, we carried out detailed *in situ* surveys of coral populations on each reef.

The first reef was dominated by large live and dead colonies of *Porites*, the remotely sensed spectra of which were readily distinguishable on the basis of their first spectral derivatives (rate of change of reflectance versus wavelength[12]) in the wavelength region 506–565 nm, as expected from *in situ* measurements[8].

The habitat of the second reef was highly heterogeneous and we used the imager to estimate the percentage cover of all substrata in ten plots of 25 $m^2$ each. Although within-plot estimates of the cover of dead *Pocillopora* coral, coralline red algae and sand varied by as much as 25–29%, estimates of live coral never differed from field data by more than 10% (Table 1). At a whole-reef (interplot) scale, estimates of the mean cover of all major benthic categories differed by less than 8%, and the cover of both live and dead coral was estimated to within 3%. There were no significant differences in estimates of mean habitat cover at the 95% confidence level (paired *t*-tests).

The video surveying methods currently used by scientific divers on the Great Barrier Reef are estimated to have a 95% probability of detecting a 10% change in live coral cover from one year to the next[13]. Power analysis of our data indicates that 22 plots of 25 $m^2$ each would need to be surveyed by remote sensing, compared with 20 equivalent-sized plots by video camera, to achieve the same level of statistical resolution on the reefs surveyed (that is, similar sample sizes for field and remote methods). However, spectographic images can be acquired over areas that are many times larger than those that can be surveyed underwater.

We anticipate that the application of multispectral remote sensing will significantly improve estimates of coral cover and changes in coral cover over time. It took us 1 hour to acquire images over 92,500 $m^2$ of reef, which represents 3,700 plots of 25 $m^2$ each, compared with 3 days to survey 10 such plots underwater. Moreover, remote images are acquired as numerical data, which can be rapidly processed electronically, reducing the time needed to generate estimates of surface cover.

**Table 1 Estimates of substrate cover for live and dead reefs**

| | Cover (%) | | Mean disparity | Maximum disparity | Minimal detectable |
|---|---|---|---|---|---|
| | Field survey | Imagery | (%) | (%) | disparity of means (%) |
| Live *Porites* | 11.5 (2.7) | 8.8 (2.9) | −2.7 | −9 | 5.6 |
| Recently dead *Porites* | 7.8 (1.6) | 6.8 (3.1) | −1.0 | 18.9 | 10.6 |
| Dead *Pocillopora* | 32.5 (8.3) | 37.2 (12.6) | 4.7 | 28.9 | 17.3 |
| Red coralline algae | 21.9 (2.4) | 15.2 (4.8) | 6.6 | −25.7 | 14.3 |
| Sand | 18.9 (6.0) | 26.8 (9.1) | 7.9 | 27.2 | 12.1 |
| *Halimeda* | 3.9 (1.6) | 5.1 (2.1) | 1.2 | −9.7 | 8.3 |

Field and remote estimates of substrate cover are shown for comparison (standard errors shown in parentheses). Results of pairwise *t*-test comparisons for each habitat were non-significant ($P < 0.05$). Minimal detectable difference represents the smallest disparity in mean cover between field and image estimates that would result in a significant *t*-test with 90% power. These values provide a worst-case scenario for the accuracy of remote sensing to predict mean habitat cover; actual disparities were considerably lower. Compact airborne spectrographic imager (CASI) data (10 bands) were corrected for depth variation (1–7 m) using image-derived attenuation coefficients. Substrata were predicted from unsupervised classification of spectral data and were categorized using independent field data. Each plot was identified on CASI images by triangulation to white plastic markers (4 $m^2$) and mapped *in situ* with a resolution of 0.01 $m^2$.


**Peter J. Mumby*, John R. M. Chisholm†, Chris D. Clark‡, John D. Hedley*, Jean Jaubert†§**

**Tropical Coastal Management Studies, Department of Marine Sciences and Coastal Management, Ridley Building, University of Newcastle upon Tyne, Newcastle upon Tyne NE1 7RU, UK*
*e-mail: p.j.mumby@ncl.ac.uk*
*†Observatoire Océanologique Européen, Centre Scientifique de Monaco, Avenue Saint-Martin, Monaco 98000, Monaco*
*‡Department of Geography and Sheffield Centre for Earth Observation Science, University of Sheffield, Sheffield S10 2TN, UK*
*§Khaled Bin Sultan Living Oceans Foundation, 1504 East Grand River, East Lansing, Michigan 48823, USA*



1. Pittock, A. B. *Am. Zool.* **39,** 10–29 (1999).
2. Kleypas, J. A. *et al. Science* **284,** 118–120 (1999).
3. Hughes, T. P. *Science* **265,** 1547–1551 (1994).
4. Harvell, C. D. *et al. Science* **285,** 1505–1510 (1999).
5. English, S., Wilkinson, C. & Baker, V. *Survey Manual for Tropical Marine Resources* (Australian Inst. Mar. Sci., Townsville, 1997).
6. Holden, H. & LeDrew, E. *Remote Sensing Environ.* **65,** 217–224 (1998).
7. Myers, M. R., Hardy, J. T., Mazel, C. H. & Dustan, P. *Coral Reefs* **18,** 179–186 (1999).
8. Clark, C. D., Mumby, P. J., Chisholm, J. R. M., Jaubert, J. & Andrefouet, S. *Int. J. Remote Sensing* **21,** 2321–2327 (2000).
9. Hochberg, E. J. & Atkinson, M. J. *Coral Reefs* **19,** 164–171 (2000).
10. Lubin, D., Li, W., Dustan, P., Mazel, C. H. & Stamnes, K. *Remote Sensing Environ.* **75,** 127–137 (2001).
11. Mumby, P. J. *et al. Mar. Biol.* **139,** 183–189 (2001).
12. Tsai, F. & Philpot, W. *Remote Sensing Environ.* **66,** 41–51 (1998).
13. Carleton, J. H. & Done, T. J. *Coral Reefs* **14,** 35–46 (1995).


Immune recognition

# A new receptor for β-glucans

The carbohydrate polymers known as β-1,3-D-glucans exert potent effects on the immune system — stimulating antitumour and antimicrobial activity, for example — by binding to receptors on macrophages and other white blood cells and activating them. Although β-glucans are known to bind to receptors, such as complement receptor 3 (ref. 1), there is evidence that another β-glucan receptor is present on macrophages. Here we identify this unknown receptor as dectin-1 (ref. 2), a finding that provides new insights into the innate immune recognition of β-glucans.

We screened a RAW264.7 complementary DNA retroviral expression library using the β-glucan-rich particle zymosan[3]

and isolated a single receptor that bound to zymosan. The DNA sequence identified the receptor as dectin-1, a small (relative molecular mass about 28,000) type-II membrane receptor with an extracellular C-type lectin-like domain fold and a cytoplasmic domain with an immunoreceptor tyrosine-based activation motif[2]. In contrast to its reported specificity for dendritic cells[2], we found that dectin-1 was expressed in every macrophage population we examined and in more tissues than was previously reported, with the highest expression being in the liver, lung and thymus (results not shown).

By assaying the ability of different carbohydrates to block the binding of zymosan to NIH3T3 cells expressing dectin-1, we found dectin-1 to be a pattern-recognition receptor that recognizes a variety of β-1,3-linked and β-1,6-linked glucans from fungi and plants (Fig. 1a). Dectin-1 did not recognize monosaccharides (data not shown) or carbohydrates with different linkages. Laminarin and glucan phosphate, a structurally defined, immunologically active β-glucan[4], were the most effective inhibitors; both bind to the β-glucan receptor on monocytes and macrophages[5,6]. The ability of dectin-1 transfectants to bind to zymosan was trypsin-sensitive, a well-known feature of the β-glucan receptor[7].

The C-type lectin-like fold of dectin-1 is similar to those of natural-killer T-cell C-type lectin domains, which lack the residues that are involved in calcium coordination and are required for carbohydrate binding in classic $Ca^{2+}$-dependent C-type lectins[8]. This is consistent with our finding that binding of dectin-1 to zymosan is independent of metal ions (results not shown).

Soluble, recombinant dectin-1 also stimulates the proliferation of T lymphocytes[2]. In a whole-cell binding assay, binding of T cells to NIH3T3 cells expressing dectin-1 was not inhibited by β-glucans (results not shown). We conclude that dectin-1 has two ligand-binding sites: one that recognizes an endogenous ligand on T cells[2], and another for exogenous carbohydrates.

The β-glucan receptor has also been implicated in the recognition and phagocytosis of intact *Saccharomyces cerevisiae*[9] and of the fungal pathogen *Candida albicans*[10]. Both of these organisms were bound to by dectin-1 transductants in a β-glucan-dependent manner (Fig. 1b), consistent with the presence of β-1,3-linked and β-1,6-linked glucans within their cell walls[11]. Dectin-1 also mediates actin-dependent phagocytosis of zymosan, an activity that requires the cytoplasmic tail of this receptor (results not shown). Furthermore, *C. albicans* conidia were internalized (Fig. 1c), showing that dectin-1 can mediate non-opsonic phagocytosis of this opportunistic pathogen.

A human homologue of dectin-1 (GenBank accession number, AY009090) is similar to the murine receptor, except that it lacks an extracellular stalk region and has no sites for *N*-linked glycosylation. Binding of zymosan and *C. albicans* by the human receptor is also dependent on β-glucan (results not shown), indicating that it may be the functional equivalent of dectin-1. Our identification of dectin-1 as the elusive macrophage receptor for β-glucan resolves a long-standing mystery and will open up new opportunities to exploit the effects of β-glucans.

**Gordon D. Brown, Siamon Gordon**

*Sir William Dunn School of Pathology, University of Oxford, South Parks Road, Oxford OX1 3RE, UK*

*e-mail: gbrown@molbiol.ox.ac.uk*

1. Ross, G. D., Cain, J. A. & Lachmann, P. J. *J. Immunol.* **134,** 3307–3315 (1985).
2. Ariizumi, K. *et al. J. Biol. Chem.* **275,** 20157–20167 (2000).
3. Di Carlo, F. J. & Fiore, J. V. *Science* **127,** 756–757 (1958).
4. Williams, D. L. *et al. Carbohydr. Res.* **219,** 203–213 (1991).
5. Muller, A. *et al. J. Immunol.* **156,** 3418–3425 (1996).
6. Mueller, A. *et al. Glycobiology* **10,** 339–346 (2000).
7. Czop, J. K. *Pathol. Immunopathol. Res.* **5,** 286–296 (1986).
8. Weis, W. I., Taylor, M. E. & Drickamer, K. *Immunol. Rev.* **163,** 19–34 (1998).
9. Giaimis, J. *et al. J. Leuk. Biol.* **54,** 564–571 (1993).
10. Janusz, M. J., Austen, K. F. & Czop, J. K. *Immunology* **65,** 181–185 (1988).
11. Bartnicki-Garcia, S. *Annu. Rev. Microbiol.* **22,** 87–108 (1968).

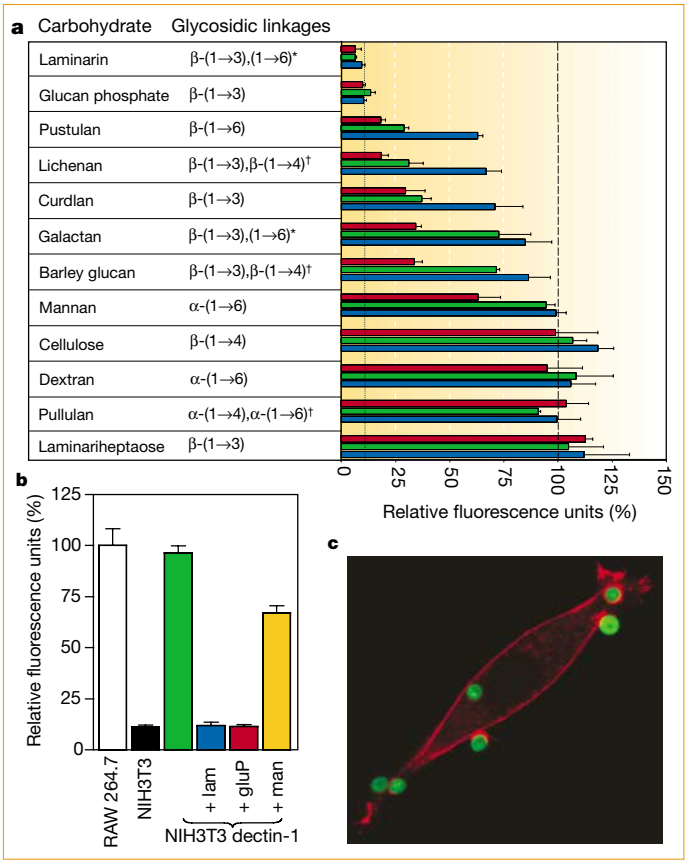


**Figure 1** Dectin-1 is a phagocytic pattern-recognition receptor that recognizes β-1,3-linked and/or β-1,6-linked glucans and intact yeast particles. **a,** Dectin-1-transduced cells were pre-treated with 500 μg $ml^{-1}$ (red bars), 100 μg $ml^{-1}$ (green bars) or 10 μg $ml^{-1}$ (blue bars) of carbohydrate before addition of fluorescently labelled zymosan particles (50 per cell). Zymosan binding was quantified by fluorometry and is expressed relative to an uninhibited control (100%; dashed line). Background binding of zymosan to untransduced NIH3T3 cells was normally about 10% (dotted line). Carbohydrates with side-chain linkages (asterisks) and/or mixed linkages (daggers) are composed of glucan polymers, except galactan (galactose monomer) and mannan (mannose monomer). **b,** Dectin-1 mediates β-glucan-dependent binding of fluorescently labelled, heat-killed *Candida albicans*, which is comparable to binding by RAW264.7 macrophages. lam, laminarin; gluP, glucan phosphate; man, mannan. **c,** Immunofluorescent micrograph of dectin-1 mediating non-opsonic phagocytosis of fluorescently labelled, heat-killed *C. albicans* (green) in NIH3T3 transductants by means of actin-based phagocytic cups (red).

Evolutionary genetics

# Clonal inheritance of avian mitochondrial DNA

We have taken a new approach to test the commonly accepted, but recently questioned, principle[1,2] of clonal inheritance of vertebrate mitochondrial DNA (mtDNA) by relating its inheritance to a female-specific marker of nuclear DNA. Whereas this is impossible in organisms with male heterogamy (such as mammals), we show here that genealogies of mtDNA and the female-specific W chromosome of a bird species are completely concordant. Our results indicate that inheritance of mtDNA is free of detectable recombination effects over an evolutionary timescale.

The avian W chromosome is small, has a low gene content, and is rich in heterochromatic, repetitive DNA. Most of the chromosome does not recombine[3], and genes in the non-recombining part are thus exclusively and clonally transmitted by females, a situation that is confirmed by the independent evolution of paralogous genes on chromosomes Z and W[4,5]. Because of this clonal inheritance, we would expect the W chromosome to segregate perfectly with mtDNA, provided that the latter is also clonally transmitted only from mother to daughter, without recombination. If this is not the case,